Title

A comprehensive analysis and source apportionment of metals in riverine sediments of a rural-urban watershed

Permalink

https://escholarship.org/uc/item/1gk0f9qr

Authors

Xia, Fang
Zhang, Chi
Qu, Liyin
et al.

Publication Date

DOI

Peer reviewed

A comprehensive analysis and source apportionment of metals in riverine sediments of a rural-urban watershed

Fang Xia[a,b,*], Chi Zhang[a], Liyin Qu[a], Qiujin Song[c], Xiaoliang Ji[a], Kun Mei[a], Randy A. Dahlgren[a,d], Minghua Zhang[a,d]

[a] Zhejiang Provincial Key Laboratory of Watershed Science and Health, Wenzhou Medical University, Wenzhou 325035, China
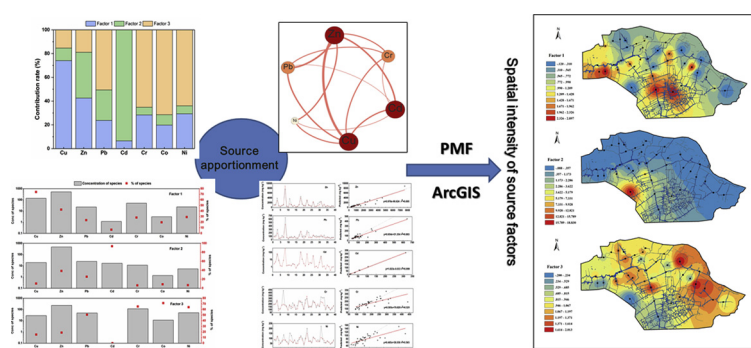[b] Key Laboratory of Environment Remediation and Ecological Health (Zhejiang University), Ministry of Education, Hangzhou 310058, China
[c] Zhejiang Dingqing Environment Detection Co. LTD, Hangzhou 325000, China
[d] Department of Land, Air and Water Resources, University of California, Davis, California 95616, United States

GRAPHICAL ABSTRACT

ARTICLE INFO

ABSTRACT

Quantitative assessment of metal sources in sediments is essential for implementation of source control and remediation strategies. This study investigated metal contamination in sediments to assess potential ecological risks and quantify pollutant sources of metals (Cu, Zn, Pb, Cd, Cr, Co and Ni) in the Wen-Rui Tang River watershed. Total and fraction analysis indicated high pollution levels of metals. Zinc and Cd posed high ecological risk based on the risk assessment code, with the highest ecological risk found in the southwestern of the watershed. The positive matrix factorization (PMF) model was highly effective in predicting total metal concentrations and identified three contributing metal sources. An agricultural source (factor 1) contributed highly to Cu (74.1%) and Zn (42.5%), and was most prominent in the west and south-central portions of the watershed. Cd (93.5%) showed a high weighting with industrial sources (factor 2) with a hot spot in the southwest. Factor 3 was identified as a mixed natural and vehicle traffic source that showed large contribution to Cr (65.2%), Ni (63.9%) and Pb (50.7%). Spatial analysis indicated a consistent pattern between PMF-identified factors and suspected metal sources at the watershed scale demonstrating the efficacy of the PMF modeling approach for watershed analysis.

* Corresponding author at: Zhejiang Provincial Key Laboratory of Watershed Science and Health, Wenzhou Medical University, Wenzhou 325035, China.
E-mail address: xiafang1988@wmu.edu.cn (F. Xia).

1. Introduction

Aquatic ecosystems often face serious metal contamination derived from rapid industrialization, urbanization, and intensive agriculture. Metal pollutants from these sources directly/indirectly accumulate in aquatic sediments impacting benthic organisms. Further, sediment is a potential threat to aquatic organisms through bioaccumulation/biomagnification of metals release to the water column. Numerous studies have reported severe contamination in soil and sediments globally (Boran and Altinok, 2010; Toth et al., 2016). For example, considerable to very high degrees of contamination by Cr, Cu, Pb and Zn were reported in Swarnamukhi River (India) sediments, which were attributed to multiple anthropogenic sources, such as residential wastes, fertilizers, pesticides and traffic activities (Patel et al., 2018). Nickel and Cr were identified to cause majority toxicity in sediments for fisheries in El Temsah Lake in the Suez Canal area (Soliman et al., 2019). Sun et al. identified Cu as the most prominent metal in urban river sediments and found the most heavily polluted area was near a petrochemical industrial complex (Sun et al., 2019). Considering the toxicity, persistence, non-biodegradability and lack of effective removal mechanisms, there is an urgent need to understand the spatial distribution, chemical fractionation, risk evaluation and contamination sources of metals in riverine sediments at the watershed scale.

Metal contamination status evaluation, ecological/health risk assessment and source identification are vital components necessary for developing effective watershed metal contamination control and remediation strategies. Numerous studies have evaluated contamination status and risk assessment of metals in sediments based on both total and various chemical fraction contents (Sundaray et al., 2011; Comero et al., 2014; Zhang et al., 2017). In particular, research has demonstrated the importance of characterizing various metal fractions for evaluating metal contamination and assessing ecological/human risk because mobile and exchangeable fractions are generally more bioaccessible and bioavailable to organisms, resulting in bioaccumulation/biomagnification in the aquatic food web (Tessier et al., 1979; Pueyo et al., 2008). For example, Ji et al. (2019) detected a high ecological risk due to an elevated exchangeable metal fraction in Baiyangdian Lake (China) and Nemati et al. (2011) identified medium and high risk for Zn and Cd in Sungai Buloh sediments by RAC index derived form a modified BCR sequential extraction procedure. Based on the perceived of the various metal fractions, several indices have been developed to provide comprehensive and reliable results for assessing potential metal toxicity risks from contaminated in sediments (Wang et al., 2019a). As an example, Siddiqui and Pandey applied a modified a modified contamination index to evaluate ecological risk associated with sediment metals at the basin-scale (Siddiqui and Pandey, 2019).

Multiple methods, including principle component analysis (PCA), correlation analysis, geographical detector method and geographically weighted regression have been applied to qualitatively identify various sources of metals in sediments (Duodu et al., 2017; Xia et al., 2018; Luo et al., 2019). These methods identify common characteristics among metals and capture the features of potential sources, for example, Giri and Singh used PCA method to recognize and extract two potential common sources of innate and anthropogenic activities for metals in surface water of the Subarnarekha River (Giri and Singh, 2014). However, quantifying contributions originating from each pollution source and the proportion contributed to each metal category cannot be obtained by these methods. The positive matrix factorization (PMF) model proposed by USEPA is recommended as an efficient receptor model for quantitative source apportionment and contribution calculation of environmental pollutants (Schwarz et al., 2019). The original contamination dataset is decomposed into a factor profile and a contribution matrix to quantify pollution sources. For example, Mehr et al. (2019) demonstrated that 85% of Zn contamination in rainwater originated from industrial sources based on PMF modeling. Further, Wang et al. (2019b) quantified four sources of metals in soils finding that

vehicle, industry, geologic and agricultural sources contributed 33.1%, 24.0%, 27.1% and 15.8%, respectively. In addition, the type of each pollution source can be inferred according to the contributions of pollutants on the source factors by PMF model. For example, Bhuiyan et al. analyzed the common characteristics of metal contaminations in water and sediments in Buriganga River and attributed them from tannery, paint, municipal, sewage, textiles and agricultural activities by applying PMF and correlation analysis (Bhuiyan et al., 2015). Most studies combined statistical analysis to confirm the reliability of PMF result, for example, Comero et al. compared PMF and PCA result of source identification of metals in Alpine lake sediments and demonstrated the comparable results from these two methods (Comero et al., 2011). There are few studies demonstrating the efficacy and spatial distribution of source apportionment of metals in soil/sediment by PMF models. Comero et al. (2014) showed the spatial distribution of source factors for Danube River sediments and found that anthropogenic sources were more prominent in tributary sediments. Thus, spatial analysis combined with PMF analysis allows exploration of detailed information concerning factors regulating metal pollutant distribution and provides advantages for effective classification and remediation of metal contaminants. However, little information is available from previous studies concerning spatial analysis from PMF results. Thus, additional investigations are required to determine the robustness of the PMF method across a wide range of metal contaminated river systems and explore the spatial influence of source factors derived from the PMF model.

Previous studies have reported spatial characteristics of metal contamination and qualitatively analyzed pollutant sources. However, little information is available to quantify contributions derived from various pollution sources or to evaluate the spatial distribution of source apportionment. Our previous studies focused on the spatial distribution and qualitative contribution of pollution sources for metals based on land-use, population, industry (Wang et al., 2019a; Xia et al., 2018; Luo et al., 2019). This study builds on our previous studies with the primary objectives of (i) conducting risk assessments based on metal chemical fractions; (ii) analyzing the correlations among metals to qualitatively identify potential pollution source by PCA and co-occurrence network; (iii) exploring source types and quantifying the proportion of various sources for each metal and (iv) characterizing the spatial influence of source intensity at the watershed scale. This study provides essential information and guidance for source control and remediation of metal contamination in riverine sediments at the watershed scale.

2. Material and methods

2.1. Study area

This research was conducted in the Wen-Rui Tang River watershed, which is a coastal watershed with drainage of ˜740 km² located in Zhejiang Province of eastern China. The river plays fundamental roles in local agriculture, industry, native fisheries/aquaculture and transportation. Mean annual temperature is ˜18 °C and annual precipitation ˜1800 mm. Sediment samples (0–10 cm) were collected in March 2017 from the mid-channel at 39 locations distributed throughout the river network (Fig. S1). The original 96 detailed land-use categories were amalgamated into six major classes based on their similarities: grass, forest, agricultural, industrial, rural and urban. Samples were collected using a clamshell bucket sampler and a well-mixed subsample was sealed in a clean polyethylene bag. Samples were stored in a cryogenic freezer (−80 °C) before freeze-drying and passing through a 100 μm nylon sieve for chemical analysis.

2.2. Metal analysis

A mixed acid digest (HNO₃-HCl-HF-HClO₄) was used to determine total metal content in sediments. Further, the modified European

Community Bureau of Reference (BCR) sequential extraction procedure was used to obtain various operationally-defined metal fractions (Unda-Calvo et al. (2017)). The extraction steps are briefly summarized as follows: (F1) 0.1 M acetic acid to extract carbonates and exchangeable metals, which represents the acid soluble fraction (Exch-); (F2) 0.5 M hydroxylamine hydrochloride to extract metals bound to Fe-Mn oxides, which represents the reducible fraction (Red-); (F3) combined 30% hydrogen peroxide and 1 M ammonium acetate to extract metals bound to organic matter, which represents the oxidizable fraction (Org-); and (F4) the mixed acid digestion (HNO_3-HCl-HF-$HClO_4$) of the residual fraction, which represent metals trapped within crystal structures of primary and secondary minerals (Res-). Detailed information concerning the BCR method can be found in Shaike et al. (2014). Total contents of Cu and Zn in extracts were determined by atomic absorption spectrometry (PinAAcle 900, Perkin-Elmer) while total contents of Pb, Cd, Cr, Co, and Ni in extracts were determined by inductively coupled plasma mass spectrometry (Agilent 8800 ICP-MS, Agilent Technologies). The GBW-07312 reference sediment (Chinese Academy of Geological Sciences) and duplicate samples were used for quality control. The relative standard deviation was ± 5% for all duplicate samples and recoveries for total metal contents in the reference sediment were 89–107%.

2.3. Risk assessment code (RAC)

Risk assessment code (RAC) is an ecological risk index based on the labile metal fraction. Previous studies have applied this index to evaluate potential risk and exchangeable fractions of metals in the environment (Sundaray et al., 2011; Zhang et al., 2017; Pejman et al., 2017). In this study, the exchangeable fraction (F1 in BCR method) was considered the labile fraction and used for the RAC calculation, which was similar to Sun et al. (2019). Ecological risk levels were divided into four levels based on the F1 proportion (Sundaray et al., 2011): low, < 10%; medium, 10–30%; high, 30–50%; and extremely high, > 50%.

2.4. Bioavailable metal index (BMI)

Due to the importance of bioavailability in ecological risk assessments of metals, the BMI was used to assess the bioavailability of metals in sediments before ecological risk assessment. In contrast to the RAC index that utilizes bioavailability for a single metal in sediment, BMI is an integrated index to assess the total bioavailability of all selected metals in sediment (Gao et al., 2018). The index was calculated following (Rosado et al., 2015):

$$BMI = (\frac{C_{F1}^1}{C_{B-F1}^1} \times \frac{C_{F1}^2}{C_{B-F1}^2} \times \cdots \times \frac{C_{F1}^n}{C_{B-F1}^n})^{1/n}$$

where n is the number of metals determined, and C_{F1}^n and C_{B-F1}^n are the F1 fractions of metal n in sediment and background sample, respectively. As the F1 content for background samples was unavailable, we assigned site B22 as the reference background samples when calculating BMI due to its relatively remote location and similar metal contents to reported background soil samples for the study region (Wang et al. (2007)).

2.5. Ratio of secondary to primary phases (RSP)

Fraction-based metal risk was assessed by chemical assessment, which is indicated by the ratio of secondary to primary metal phases. In this research the secondary phase was considered the sum of F1, F2 and F3, while the primary phase was represented by F4. Therefore, RSP was calculated as follows (Lin et al., 2014):

$$P = \frac{F1 + F2 + F3}{F4}$$

where F1, F2, F3 and F4 are fractions extracted by the BCR method. Contamination levels were divided into 4 categories according to calculated P values: no risk, P < 1; low risk, $1 \leq P < 2$; medium risk, $1 \leq P < 2$; and high risk, $P \geq 3$.

2.6. Positive matrix fractionalization (PMF)

PMF, a typical receptor model, was used for metal pollution source apportionment (Mehr et al., 2019; Zhi et al., 2016). This model was used to factorize the metal dataset into two matrices using the following formula:

$$x_{ij} = \sum_{k=1}^{p} g_{ik} f_{kj} + e_{ij}$$

where x_{ij} is metal concentration matrix; i is ith sampling site; j is metal j; p is the source number; g_{ik} is factor contribution to the sample; f_{kj} is pollution source profile (factors); and e_{ij} is residual matrix.

Factor contribution g_{ik} and pollution source profile f_{kj} were determined by minimizing the PMF model's object function Q (Paatero, 1997):

$$Q = \sum_{i=1}^{n} \sum_{j=1}^{m} (\frac{e_{ij}}{u_{ij}})^2$$

where u_{ij} represents the uncertainty for metal j at sampling site i.

The uncertainty calculation follows the function:

$$u_{ij} = \begin{cases} \frac{5}{6} \times MDL & x_{ij} \leq MDL \\ \sqrt{(\sigma_j \times x_{ij})^2 + (0.5 \times MDL)^2} & x_{ij} > MDL \end{cases}$$

where σ_j represents the relative standard deviation for metal j.

In this study, 7 metals in 39 sediments were included in the PMF calculation. EPA PMF model (ver. 5.0) was used to quantify the metals source in sediments from the Wen-Rui Tang River watershed. Detailed information for input files and uncertainty calculation for metal data can be found in previous reports (Paatero, 1997; Paatero and Hopke, 2009; U.S. Environmental Protection Agency, 2019).

2.7. Co-occurrence network

To visualize correlations among metals in sediments, co-occurrence networks were generated by Gephi (ver. 0.9.2), which is based on Spearman's correlation coefficient analysis. To assure robust correlations among entities, the Spearman's ρ was set at > 0.6 with a statistically significance of p < 0.01 (Barberán et al., 2012).

3. Results and discussion

3.1. Metal concentrations and chemical fraction in sediments

The mean ± std (range) concentrations (mg kg^{-1}) for Cu, Zn, Pb, Cd, Cr, Co and Ni in sediments were 310 ± 804 (29.5–5093), 1361 ± 1475 (263–7616), 115 ± 107 (34.5–644), 17.7 ± 53.7 (0.34–314), 192 ± 77.2 (94.2–440), 17.0 ± 4.7 (9.79–32.0), and 89.0 ± 39.9 (38.1–223.8), respectively (Fig. S2). In general, sediments were highly contaminated by some metals in the investigated watershed when compared to soil background values (Wang et al., 2007). Except for Co, the exceedance rates of the sites for total metal concentrations compared to background levels were 92–100%. The most prominent metal was Cd, which was ˜100× times higher than background, followed by Zn and Cu (˜10× times). Cobalt had a lower occurrence of contamination with only 64.1% exceeding background levels and only five sampling sites having concentrations greater than 150% of the background level. Spatial distribution for some metals was reported in our previous work (Xia et al., 2018) while Co and Ni are shown in Fig S3 as Supplementary information. In general, several
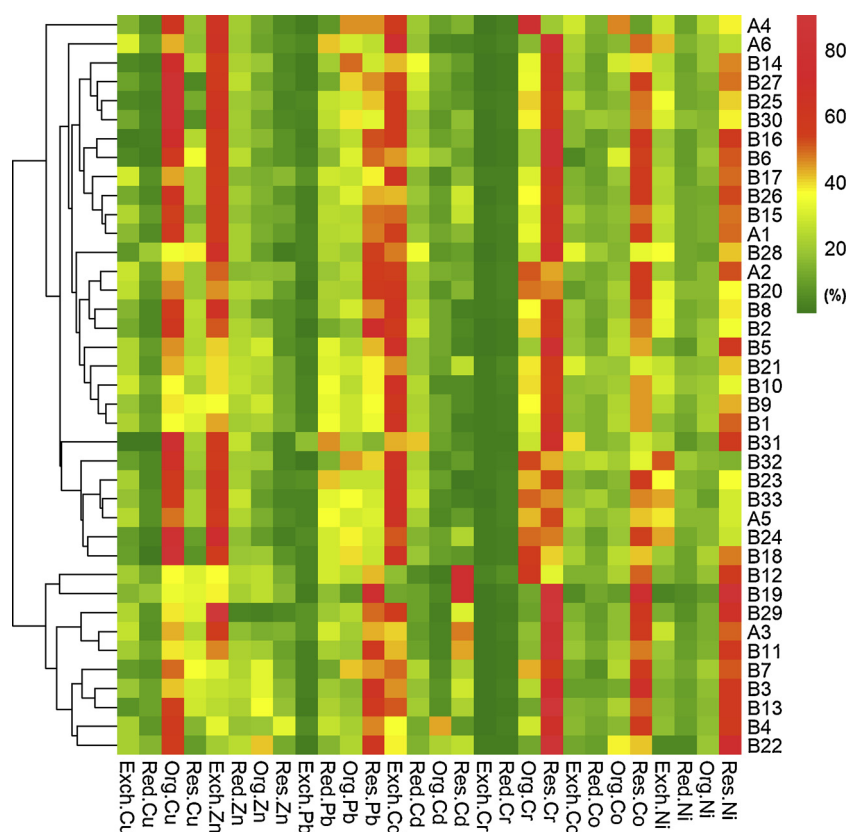
Fig. 1. Metal fractions in sediments for 39 sampling sites in Wen-Rui Tang River watershed.

distinct 'hot spots' were identified in the spatial patterns. Hot spots for Zn, Pb and Cd were found in the southwest, Cu in the east and Ni in the northern portion of the watershed. In contrast, Co did not show any distinct spatial patterns. The extremely high concentrations associated with these hot spot sites were mainly located in the vicinity of industrial parks. The high total metal contents and high spatial variability are indicative of anthropogenic inputs to the riverine sediments. Most of these metals can be linked to local industrial wastes and wastewater originating from electroplating, printing, dye chemicals and synthetic leather industries/domestic workshops that have been active in this watershed over the past few decades. These industrial effluents contain high concentration of metals, including Zn, Pb and Cd (Shomar, 2009). Due to rapid industrial development in the watershed, industrial effluents are often directly discharged to the river system with no wastewater treatment. In contrast to other metals, Co concentrations were similar to background levels and showed no apparent spatial patterns, implying that Co primarily originated from natural source.

The BCR-derived metal fractions impacting bioavailability and bioaccessibility are summarized in Fig. 1. Zinc and Cd were dominantly found in the exchangeable fraction (F1), while Pb, Cr, Co and Ni were concentrated in the residual fraction (F4). The average Exch-Zn and Exch-Cd percentages were 51.6% (range: 20.9–90.4%) and 52.2% (range: 11.2–74.5%), respectively. Previous studies demonstrated that the elevated proportions of exchangeable metals originated primarily from human sources (Ji et al., 2019; Otansev et al., 2016) proving support for anthropogenic inputs as the primary source of Zn and Cd in the study watershed. The chemical fractions for Cu showed a distinct distribution from the other metals. Copper was primarily associated with F3 with a mean of 54.3% (range of 34.4–82.9%). While previous studies have demonstrated a strong affinity between Cu and organic ligands (Bruder-Hubscher et al., 2002), there was no significant correlation between Cu and organic C concentrations in this study. The remaining metals were most abundant in the residual fraction (F4):

Pb = 43.8%, Cr = 62.4%, Co = 48.6% and Ni = 46.9%. The large proportion associated with F4 suggests a relatively lower ecological risk as these metals are primarily incorporated with crystalline silicate lattices of primary minerals (Zhang et al., 2017).

The RSP index was calculated as a measure of metal contamination (Fig. 2). The RSP for Zn exceeded 3 in more than 90% of the sites, indicating a high pollution level throughout the watershed. The percentage of sites with high pollution level for Cd and Cu were 74.4% and 69.2%, respectively. In contrast, metal pollutant levels were lower for Pb with 51.3% sites having low pollution and 25.6% no apparent accumulation. More than 80% of sites had low to no pollution levels for Co and Ni, while Cr had no apparent pollution levels for most sampling sites. Generally, metal pollution based on the RSP index followed: Zn > Cd > Cu > Pb > Ni ≈ Co > Cr. The high RSP values for Zn, Cd and Cu are consistent with the high total metal contents compared to their background values in the watershed. Cobalt showed slight pollution, which was coincident with its relatively low total concentrations. In contrast, RSP values for Pb, Ni and Cr indicated low-to-none pollution, while their total metal concentrations were highly elevated compared to their background levels. This somewhat contradictory result is attributed to differences in the distribution of chemical fractions among these metals. Total Pb, Cr and Ni concentrations at most sites exceeded background levels, but the majority of metals resided in F4. In contrast, Zn, Cd and Cu had both high total metal contents and a high proportion of available/accessible fractions (F1 + F2 + F3). These results highlight the importance of incorporating metal fractionation methods into evaluating pollution levels and risks of metals in the environment (Gusiatin and Kulikowska, 2014).

3.2. Ecological risk assessment based on metal fractions

Several studies have previously assessed ecological risk of metals in sediments (Zhang et al., 2017; Duodu et al., 2017) and we previously
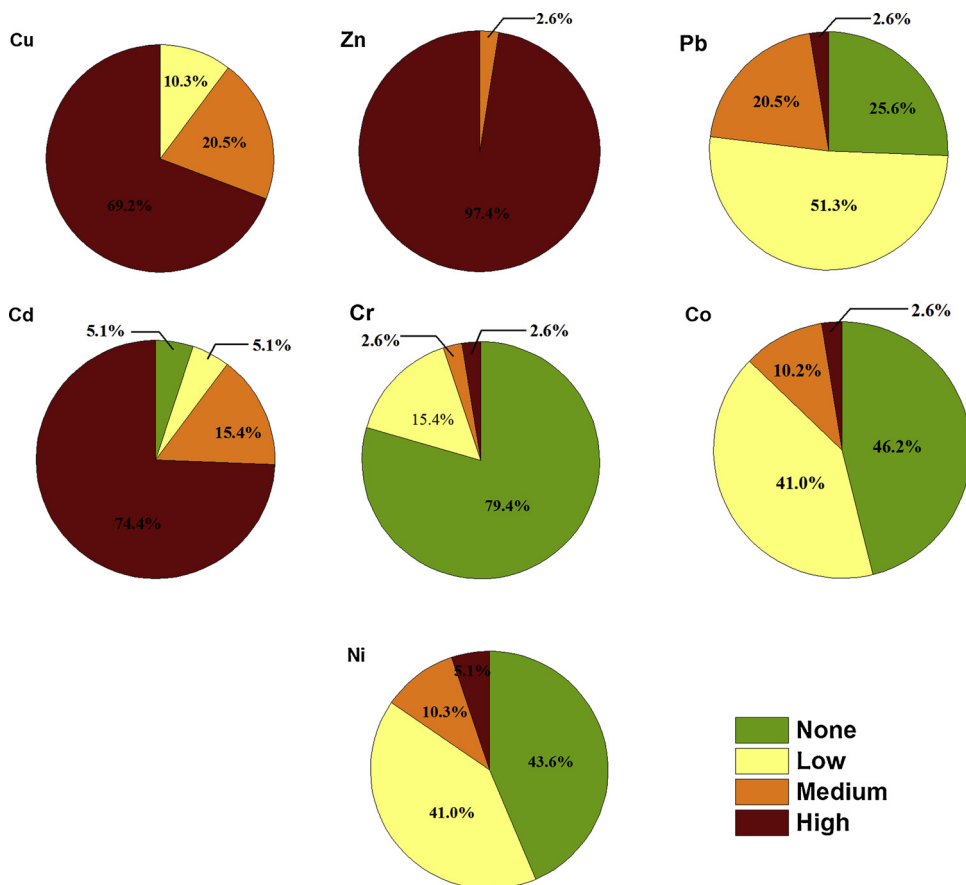
Fig. 2. Percentage of metal contamination levels in sediments represented by ratio of secondary to primary phases (RSP) in sediments.
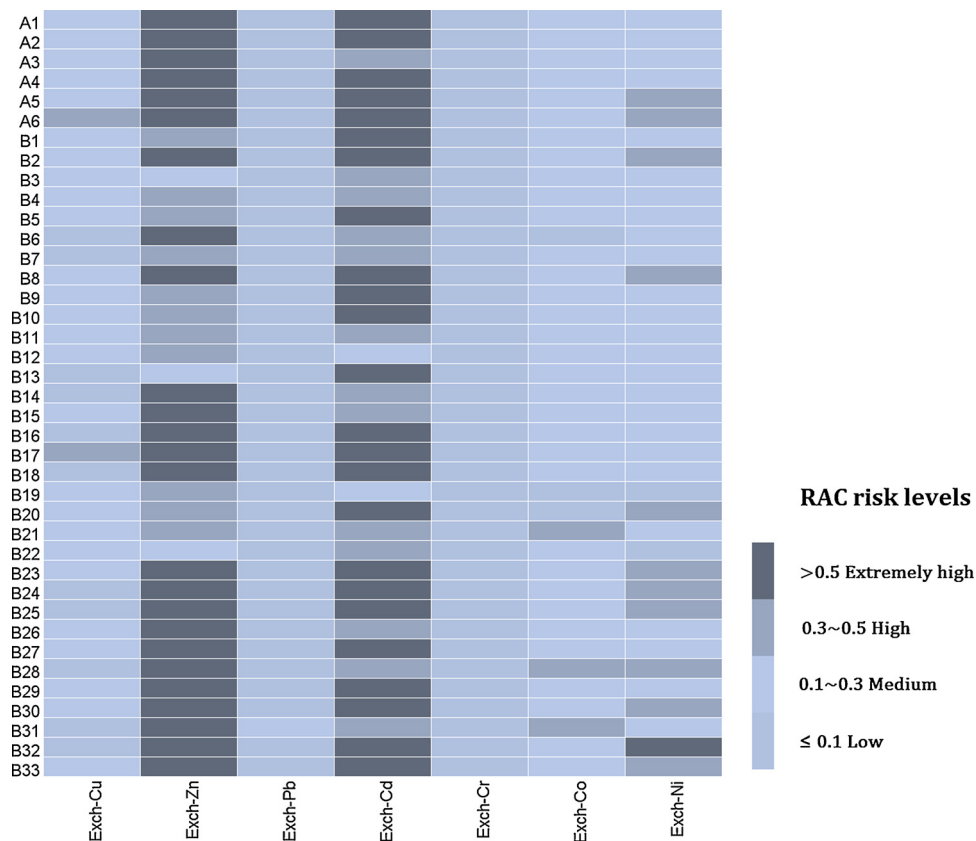

Fig. 3. Heatmap of RAC risk assessment for sampling sites.

reported ecological risks based on total metal contents in various land-use clusters for this watershed (Siddiqui and Pandey, 2019). As described above, chemical metal fractions showed large variation throughout the watershed, resulting in a considerable discrepancy for ecological risk when compared to metrics based on total metal content. The F1 fraction is defined as the fraction most easily accessible to organisms thereby posing the most potential for adverse ecological and human-health risk. Risk assessment code (RAC) is used to assess the ecological risk by comparing the F1 proportion to various RAC risk levels. The average percentage of the exchangeable fraction relative to total metal concentration followed: Cd (52.2%) ≈ Zn (51.6%) > Ni (25.4%) > Co (17.9%) > Cu (16.5%) > Pb (3.5%) > Cr (1.1%). Generally, Cd and Zn showed extremely high ecological risk, while Ni, Co and Cu were identified with medium risk. In contrast, Pb and Cr displayed low risk. In addition, ecological risk by RAC showed spatial differences among sites. Most sites showed extremely high risk for Zn and Cd due to their high exchangeable fraction (Fig. 3). Sites A6 and B17 showed high risk for Cu while more than half of the sites showed a medium risk. Cobalt and Ni showed overall medium risk at most sampling sites. However, Ni displayed extremely high risk at site B32 due to its high exchangeable fraction. In contrast, Pb and Cr showed consistently low risk throughout all the sites in the watershed as a result of a high proportion of the residual fraction. These results clearly demonstrate that Cd and Zn posed the highest ecological risk within the watershed.

RAC assesses ecological risk for a single metal, but does not provide an integrated index of risks for all metals. Therefore, we applied BMI to assess the integrated ecological risk associated with all the metals; this method is commonly used to evaluate metal pollution and risk in the environment. B22 was assigned as the reference site due to its remote location and its overall metal concentrations being comparable to background levels. The average BMI was 6.2, ranging from 1.3 at site B13 to 19.3 at site B28. Notably, sites A4, A5, B25, B28 and B31stood out with high BMI values of 15.8, 14.3, 14.3, 19.3 and 15.5, respectively. There is no specific threshold value to evaluate risk levels for BMI; however, Omwene et al. (Omwene et al. (2018)) demonstrated pollution risk when PLI index values were greater than 1, which involves a similar calculation to BMI. As a result, the investigated watershed contains areas with potentially high ecological risk. A detailed spatial analysis showed BMI generally decreasing from south to north and the sites with highest BMI values were mainly located in the southwest portion of the watershed (Fig. 4). BMI values were compared to the exchangeable metal fractions to examine reliability between assessment metrics. Sites with high BMI values had a high proportion of
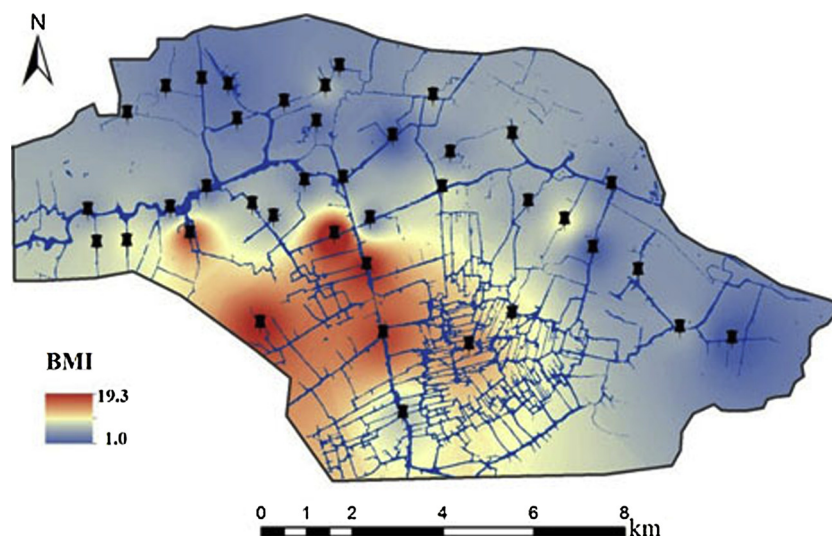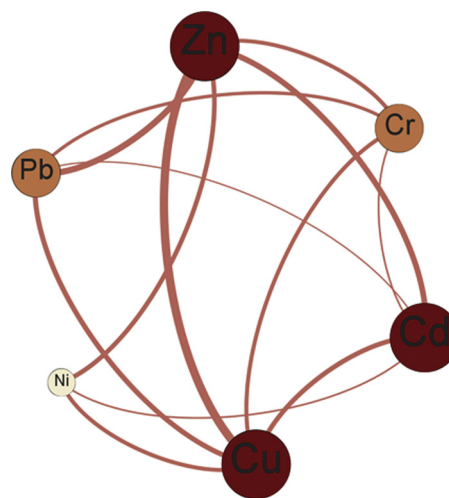

Fig. 5. Co-occurrence network of metals in sediments (Spearman's ρ > 0.6 and p < 0.01). Nodes represent metals while the connections between two nodes represent correlation coefficient between them. The size of each node is proportional to the correlations while the thickness of each connection is proportional to the Spearman's correlation coefficients.

Exch-Zn (Spearman correlation coefficient: 0.800, p < 0.01) and Exch-Cd (0.828, p < 0.01), confirming a similar spatial pattern between BMI and exchangeable fractions for these metals within the sediments. These results highlight the large contribution of Zn and Cd to local ecological risk and the consistency between RAC and exchangeable metal fractions in identifying potential ecological risks.

3.3. Principle component analysis and co-occurrence network

PCA analysis is a typical method used to identify common characteristics and recognize potential sources of metals (Zhi et al., 2016; Kang et al., 2017). In addition, PCA analysis assists with determining the number of factors for PMF models. In this study, PCA was applied for total metal concentrations and three components were identified based on their eigenvalues that explained 83.5% of the total variance (Table S1). Zinc, Pb and Cd showed high loading on PC1 (45.4% of the total variance), indicating a similar pollution source within the watershed. Similar spatial distribution patterns were found in our previous work (Xia et al., 2018). Chromium and Ni had high loading on PC2 (24.2% of the total variance), while Cu had a high loading on PC3
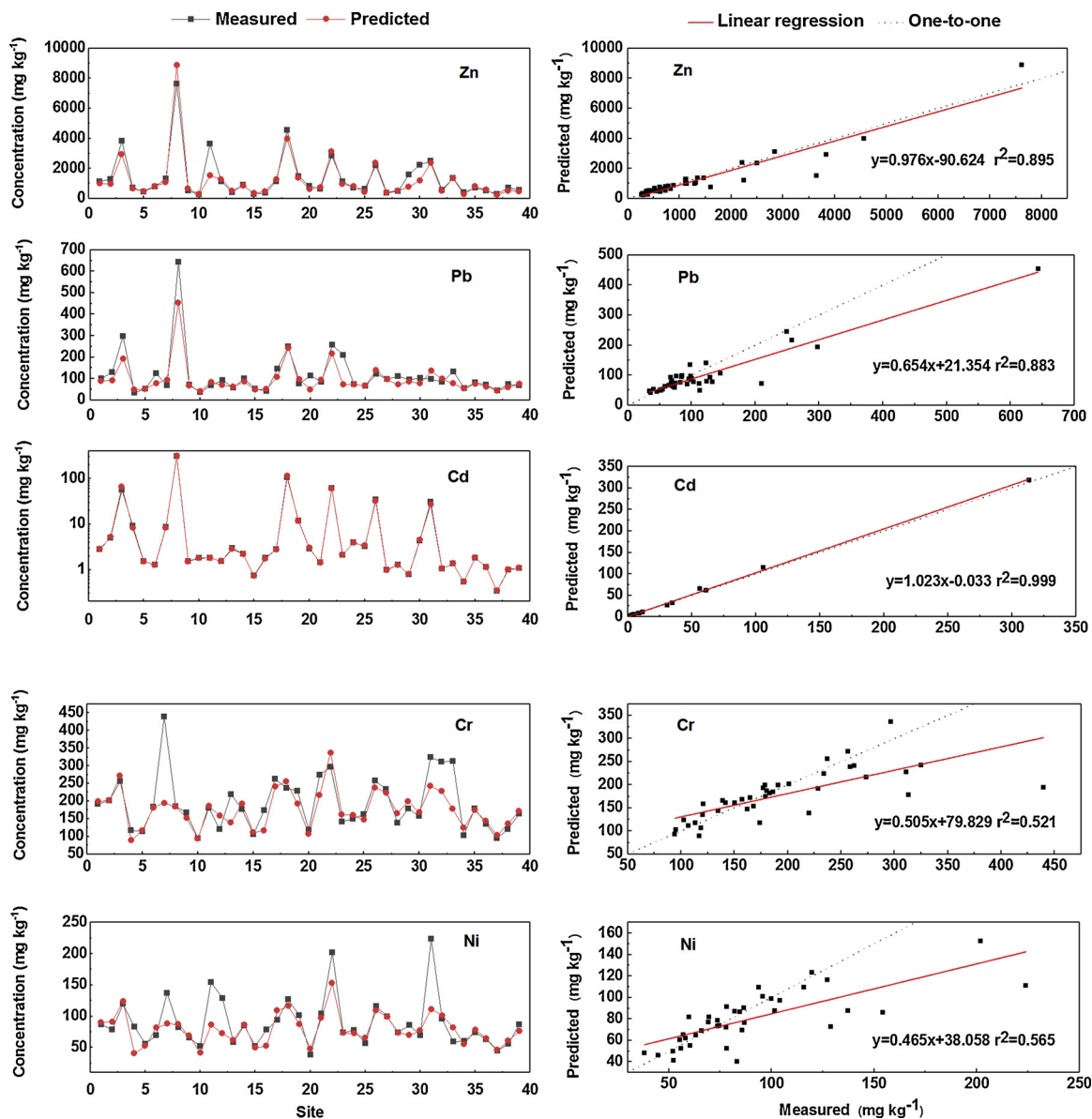

Fig. 4. Spatial distribution of ecological risk evaluated by BMI method.

Fig. 6. Concentrations of measured and predicted metals in sediments (left panels). Black lines represent measured concentrations and red lines represent predicted concentrations. Linear regression results are compared to one-to-one function line (y = x) in the right panels. Black dashed lines represent one-to-one function while red lines represent linear regression result. (For interpretation of the references to colour in this figure legend, the reader is referred to the web version of this article).

Table 1
Source contribution for metals in sediment by the PMF model.

Element	Profile contribution (mg kg⁻¹)			Percentage contribution (%)		
	Factor 1	Factor 2	Factor 3	Factor 1	Factor 2	Factor 3
Cu	137.5	19.6	28.5	74.1	10.6	15.3
Zn	527.7	479.1	234.4	42.5	38.6	18.9
Pb	23.0	24.8	49.1	23.7	25.6	50.7
Cd	1.17	16.9	0	6.5	93.5	0
Cr	50.2	11.5	115.6	28.3	6.5	65.2
Co	3.1	1.4	11.2	19.8	8.8	71.4
Ni	23.5	5.4	51.3	29.3	6.8	63.9

(15.7% of the total variance). To further assess common sources among the metals, we performed a co-occurrence network (Liu et al., 2015). Spearman's correlation coefficients (> 0.6) between metals were used to construct the co-occurrence network (Fig. 5), which indicated significant correlations between theses metals. Cobalt was excluded from

the co-occurrence network due to its weak or non-significant correlations with the other metals. Significant co-occurrence correlations were determined among metals, especially for Zn, Cd and Cu (Fig. 5). Copper had high co-occurrence correlations with all the other metals, except Co. Lead and Cr showed similar co-occurrence correlations with Cu, Zn
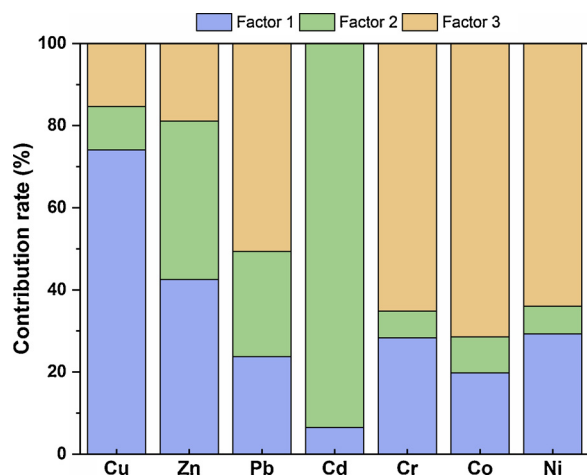
Fig. 7. Contribution of different factors for each metal determined by the PMF model.

and Cd. Nickel showed relatively low co-occurrence correlations with all the other metals. High co-occurrence correlations among metals are suggestive of common anthropogenic sources, such as industrial waste discharge or agricultural activities.

3.4. Assessment of metal sources by PMF model

The PMF model was used to identify possible sources of metals in sediments in Wen-Rui Tang River watershed. Metal concentrations and their corresponding uncertainty data were used as inputs to the PMF model. As Co was near background level and posed none to low ecological risk in the watershed, it was set as weak in the base model run and the detailed results for Co was ignored. Based on results of the PCA analysis, the number of factors for the base model run was set to three. Three factors were identified as the optimum number of factors for this metal dataset based on minimization of Q values and r^2 values between measured and predicted metal concentrations. Most sites were determined with absolute residual values lower than 3 for measured and predicted metal concentrations.

Predicted metal concentrations from the PMF model were compared with measured concentrations (Figs. 6 and S4) and determination coefficients (r^2) were used to evaluate the efficacy of model predictions. Most metals showed reasonable linear regression results with r^2 values greater than 0.52. The higher r^2 values were found for Zn (0.895), Pb (0.883) and Cd (0.999), indicating that the metal concentrations predicted by the selected source factors in the PMF model were well explained. The r^2 values for Cu was only 0.129 when all the data were included; however, this analysis was strongly influenced by a single outlier at site 18 (5092.5 mg kg^{-1} and 27 × average Cu concentration). Following removal of this outlier, the r^2 values increased to 0.961, indicating a significant and disproportional influence of the outlier to PMF prediction results (Men et al., 2019). Similarly, spatial analysis indices, such as Moran's I is sensitive to outliers, but is strongly indicative of contaminated locations (Zhao et al., 2014, 2019). Abnormal events commonly create outlier values in air pollution source apportionment investigations, such as fire and fireworks, and the PMF model is highly sensitive to these outliers (Norris et al., 2008). Site B18 was located in the urban region surround by commercial and residential areas, where no unique point source can be currently identified. The extremely high Cu concentration may be attributed to an unexpected legacy source and therefore not associated with current land-use activities.

Details of the PMF result for factor profiles are shown in Table 1 and Fig. S5. Factor 1 was strongly characterized by Cu and had a 74.1% contribution. Zinc, Pb and Cr showed a contribution by factor 1 of

42.5%, 23.7% and 28.3%, respectively. Factor 2 was predominantly represented by Cd with a 93.5% contribution. Factor 2 also showed a medium contribution to Zn and Pb. These are primary metals attributed to local industrial emissions, thus factor 2 probably represents an industrial pollution source. Factor 3 was represented by Pb, Cr, and Ni with contributions of 50.7%, 65.2% and 63.9%, respectively. The overall contributions from each source factor to the various metals are summarized in Fig. 7. Combined with the PMF profile results (Table 1), Cr and Ni showed similar source components while Zn and Pb shared similar factors in their source contributions. In contrast, Cu was predominantly contributed by a single factor. The results from the PMF model were generally consistent with the PCA analysis. For example, Cr and Ni had high loadings on PC2 while they showed a high weighting with factor 3 of the PMF analysis. The consistency between the two approaches provides strong support for Cr and Ni sharing a similar source. Similar results were also found for Zn and Pb. Cu was highly characterized by factor 1 in the PMF analysis and showed high loading on PC3, indicating a distinct source compared to the other metals. The high levels of Cu in riverine sediments may be attributed to fertilizer, pesticides and feed supplements associated with agricultural activities in the watershed. Thus, factor 1 is most likely dominated by agricultural emissions. Cd displayed some inconsistent results with the predominant weighting in PMF factor 2 contrasting with results from PCA and co-occurrence network analysis. The inconsistency may be attributed to Cd being from a predominant industrial source for factor 2 that will be discussed with the combination of spatial intensity of source factors in the next section.

3.5. Spatial intensity of source factors by PMF model

According to the contribution of PMF-derived source factors to metal concentrations at each site, inverse distance weighting in ArcGIS was used to predict spatial distribution patterns for these source factors across the watershed (Fig. 8). Factor 1 strongly characterized Cu along with medium weighting for Zn, Pb and Cr. Generally, two high-level areas were identified for factor 1, in the west and central-south portion of the watershed. Notably, sampling sites B32, B24 and A5 were identified as having a high value for factor 1. These sites with high Cu concentration were mainly located in rural and agricultural land-use areas within the watershed. Thus, we inferred that source factor 1 was mainly related to agricultural activities, such as fertilizer, pesticides and domestic animal feed supplements, which resulted in Cu accumulation in the sediments (Song et al., 2018; Guan et al., 2018).

Cadmium was strongly associated with factor 2 (Fig. 7). A Cd hot spot was identified in the southwestern portion of the watershed with sites B31 and B28 also having high values for Cd and Zn (Fig. 8). This high-level area was located in close proximity to an industrial park from which contaminated wastewater was directly discharged into the river in recent decades. As a result, we infer that factor 2 is primarily associated with Cd originating from industrial sources.

Factor 3 was most strongly associated with Cr, Co and Ni, which all showed a similar contribution of source factors dominated by factor 3. Spatial differences for the intensity in factor 3 throughout the watershed were relatively small, with the exception of a few specific sites (Fig. 8). The lack of a distinct spatial trend indicates a more homogeneous spatial distribution pattern of these metals at the watershed scale. The highest values for factors 3 were found at sites B19 and B11 in the northeastern portion of the watershed. These sites were characterized by high concentrations of Co, Cr and Ni and were mainly located in urban areas. Previous studies indicated that Cr and Ni were often inherited from geologic materials (Rodríguez Martín et al., 2006; Xue et al., 2014). Chromium and Ni were generally comparable to the background values of soils in the watershed. Lead also showed a relatively strong association (49.1%) with factor 3 (Table 1). Previous studies have identified Pb as originating primarily from vehicle traffic sources that are concentrated in the urban district (Li et al., 2016;
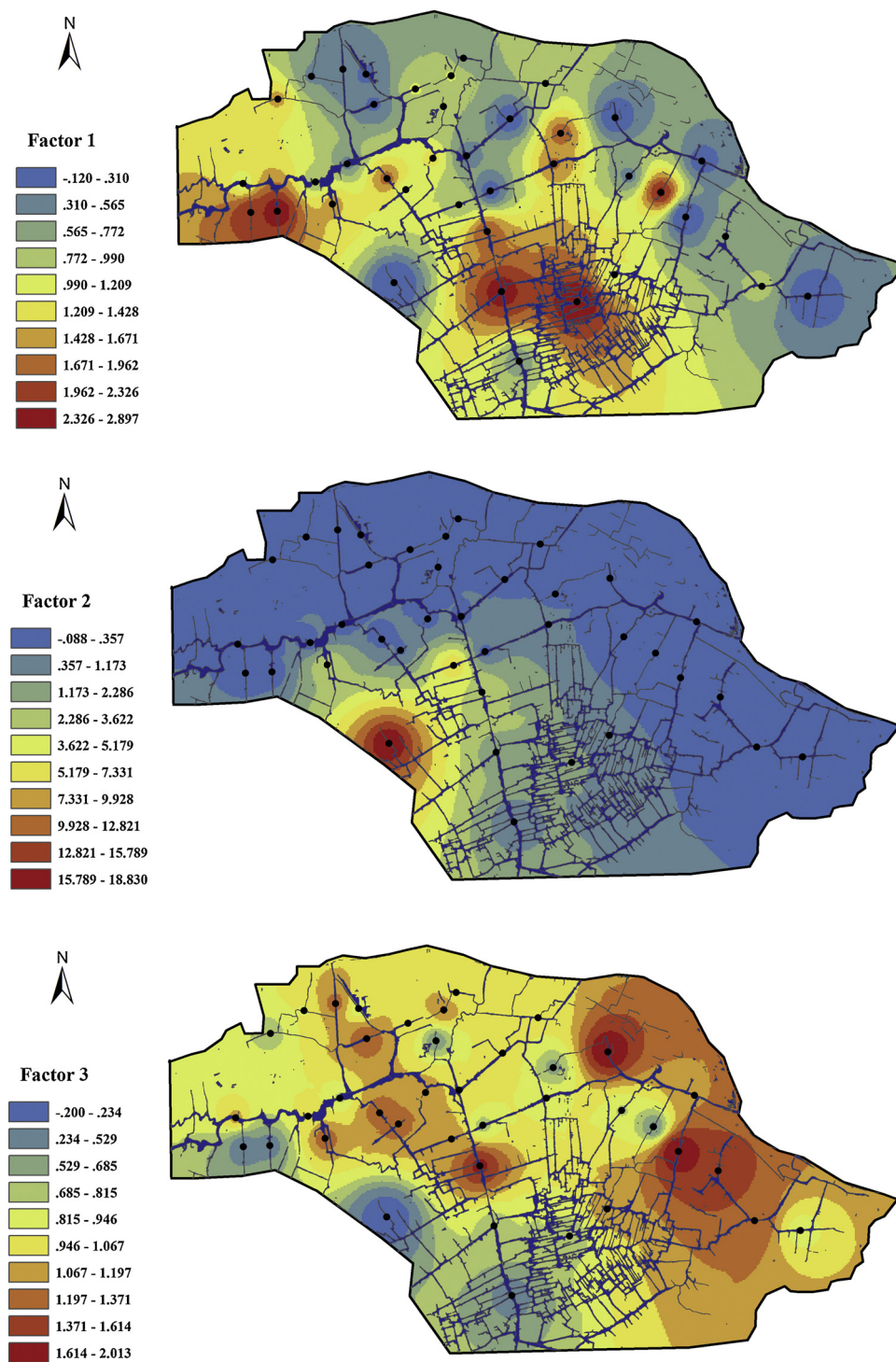
Fig. 8. Spatial distribution of source factor intensities for metals in sediments.

Murajanum et al., 2007). Thus, we interpret that factor 3 reflects a combination of natural background metals and traffic sources within watershed.

4. Conclusions

Riverine sediments in the Wen-Rui Tang watershed were contaminated by metals that resulted in potential risks to aquatic ecosystems and human health, based on indices related to both total concentrations and chemical fractions. Notably, Zn and Cd showed high ecological risk due to a high proportion of F1 fraction, and the

southwestern portion of the watershed was identified with higher risks based on BMI calculation. PMF analysis demonstrated good prediction ability for most metals with determination coefficients for linear regressions in the range 0.521–0.999, and three main source factors were extracted by the PMF model. Copper was mainly contributed by agricultural sources (74.1%), while Cd was largely characterized by industrial sources (93.5%). Zinc received relatively equal contributions from agricultural (42.5%) and industrial (38.6%) sources. A mixed geologic and traffic source was dominant for Cr, Ni and Pb with contributions of 65.2%, 63.9% and 50.7%, respectively. Spatially, the agricultural source (factor 1) mainly impacted the west and south-

central portions of the watershed, while the industrial source (factor 2) occurred as 'hot spot' in the southwest. The mixed source (factor 3) mainly influenced the urban areas. Results from this study provided important information for guiding source control and remediation strategies of metal contamination at the watershed scale.

Declaration of Competing Interest

None.

Acknowledgments

Appendix A. Supplementary data

Supplementary material related to this article can be found, in the online version, at doi:https://doi.org/10.1016/j.jhazmat.2019.121230.

References

Barberán, A., Bates, S.T., Casamayor, E.O., Fierer, N., 2012. Using network analysis to explore co-occurrence patterns in soil microbial communities. ISME J. 6, 343–351. https://doi.org/10.1038/ismej.2011.119.

Bhuiyan, M.A.H., Dampare, S.B., Islam, M.A., Suzuki, S., 2015. Source apportionment and pollution evaluation of heavy metals in water and sediments of Buriganga River, Bangladesh, using multivariate analysis and pollution evaluation indices. Environ. Monit. Assess. 187, 4075. https://doi.org/10.1007/s10661-014-4075-0.

Boran, M., Altinok, I., 2010. A review of heavy metals in water, sediment and living organisms in the Black Sea. Turk. J. Fish. Aquat. Sci. 10, 565–572. https://doi.org/10.4194/trjfas.2010.0418.

Bruder-Hubscher, V., Lagarde, F., Leroy, M.J.F., Coughanowr, C., Enguehard, F., 2002. Application of a sequential extraction procedure to study the release of elements from municipal solid waste incineration bottom ash. Anal. Chim. Acta 451, 285–295. https://doi.org/10.1016/S0003-2670(01)01403-9.

Comero, S., Vaccaro, S., Locoro, G., De-Capitani, L., Gawlik, B.M., 2014. Characterization of the Danube River sediments using the PMF multivariate approach. Chemosphere 95, 329–335. https://doi.org/10.1016/j.chemosphere.2013.09.028.

Comero, S., Locoro, G., Free, G., Vaccaro, S., De Capitani, L., Gawlik, B.M., 2011. Characterisation of Alpine lake sediments using multivariate statistical techniques. Chemometr. Intell. Lab. 107, 24–30. https://doi.org/10.1016/j.chemolab.2011.01.002.

Duodu, G.O., Goonetilleke, A., Ayoko, G.A., 2017. Potential bioavailability assessment, source apportionment and ecological risk of heavy metals in the sediment of Brisbane River estuary, Australia. Mar. Pollut. Bull. 117, 523–531. https://doi.org/10.1016/j.marpolbul.2017.02.017.

Gao, L., Wang, Z.W., Li, S.H., Chen, J.Y., 2018. Bioavailability and toxicity of trace metals (Cd, Cr, Cu, Ni, and Zn) in sediment cores from the Shima River, South China. Chemosphere 192, 31–42. https://doi.org/10.1016/j.chemosphere.2017.10.110.

Giri, S., Singh, A.K., 2014. Risk assessment, statistical source identification and seasonal fluctuation of dissolved metals in the Subatnarekha River, India. J. Hazard. Mater. 265, 305–314. https://doi.org/10.1016/j.jhazmat.2013.09.067.

Guan, Q.Y., Wang, F.F., Xu, C.Q., Pan, N.H., Lin, J.K., Zhao, R., Yang, Y.Y., Luo, H.P., 2018. Source apportionment of heavy metals in agricultural soil based on PMF: a case study in Hexi Corridor, northwest China. Chemosphere 193, 189–197. https://doi.org/10.1016/j.chemosphere.2017.10.151.

Gusiatin, Z.M., Kulikowska, D., 2014. The usability of the IR, RAC and MRI indices of heavy metal distribution to assess the environmental quality of sewage sludge composts. Waste Manage. 34, 1227–1236. https://doi.org/10.1016/j.wasman.2014.04.005.

Ji, Z.H., Zhang, Y., Zhang, H., Huang, C.X., Pei, Y.S., 2019. Fraction spatial distributions and ecological risk assessment of heavy metals in the sediments of Baiyangdian Lake. Ecotox. Environ. Safe. 174, 417–428. https://doi.org/10.1016/j.ecoenv.2019.02.062.

Kang, X.M., Song, J.M., Yuan, H.M., Duan, L.Q., Li, X.G., Lin, N., Liang, X.M., Qu, B.X., 2017. Speciation of heavy metals in different grain sizes of Jiaozhou Bay sediments: Bioavailability, ecological risk assessment and source analysis on a centennial timescale. Ecotox. Environ. Safe. 143, 296–306. https://doi.org/10.1016/j.ecoenv.2017.05.036.

Li, F., Zhang, J.D., Huang, J.H., Huang, D.W., Yang, J., Song, Y.W., Zeng, G.M., 2016. Heavy metals in road dust from Xiandao District, Changsha City, China: Characteristics, health risk assessment, and integrated source identification. Environ. Sci. Pollut. Res. 23, 13100–13113. https://doi.org/10.1007/s11356-016-6458-y.

Lin, C., Liu, Y., Li, W.Q., Sun, X.W., Ji, W.D., 2014. Speciation, distribution, and potential ecological risk assessment of heavy metals in Xiamen Bay surface sediment. Acta Oceanolog. Sin. 33, 13–21. https://doi.org/10.1007/s13131-014-0453-2.

Liu, L.L., Wang, Z.P., Ju, F., Zhang, T., 2015. Co-occurrence correlations of heavy metals in sediments revealed using network analysis. Chemosphere 119, 1305–1313. https://doi.org/10.1016/j.chemosphere.2014.01.068.

Luo, L.L., Mei, K., Qu, L.Y., Zhang, C., Chen, H., Wang, S.Y., Di, D., Huang, H., Wang, Z.F., Xia, F., Dahlgren, R.A., Zhang, M.H., 2019. Assessment of the Geographical Detector Method for investigating heavy metal source apportionment in an urban watershed of Eastern China. Sci. Total Environ. 653, 714–722. https://doi.org/10.1016/j.scitotenv.2018.10.424.

Mehr, M.R., Keshavarzi, B., Sorooshian, A., 2019. Influence of natural and urban emissions on rainwater chemistry at a southwestern Iran coastal site. Sci. Total Environ. 668, 1213–1221. https://doi.org/10.1016/j.scitotenv.2019.03.082.

Men, C., Liu, R.M., Wang, Q.R., Guo, L.J., Miao, Y.X., Shen, Z.Y., 2019. Uncertainty analysis in source apportionment of heavy metals in road dust based on positive matrix factorization model and geographic information system. Sci. Total Environ. 652, 27–39. https://doi.org/10.1016/j.scitotenv.2018.10.212.

Murajanum, M., Nakajima, F., Furumai, H., Tomiyasu, B., Owari, M., 2007. Identification of particles containing chromium and lead in road dust and soakaway sediment by electron probe microanalyser. Chemosphere 67, 2000–2010. https://doi.org/10.1016/j.chemosphere.2006.11.044.

Nemati, K., Bakar, N.K.A., Abas, M.R., Sobhanzadeh, E., 2011. Speciation of heavy metals by modified BCR sequential extraction procedure in different depths of sediments from Sungai Buloh, Selangor, Malaysia. J. Hazard. Mater. 192, 402–410. https://doi.org/10.1016/j.jhazmat.2011.05.039.

Norris, G., Vedantham, R., Wade, K., Brown, S., Prouty, J., Foley, C., 2008. EPA Positive Matrix Factorization (PMF) 3.0 Fundamentals & User Guide. US Environmental Protection Agency Office of Research and Development, Washington, DC.

Omwene, P.I., Öncel, M.S., Celen, M., Kobya, M., 2018. Heavy metal pollution and spatial distribution in surface sediments of Mustafakemalpasa stream located in the world's largest borate basin (Turkey). Chemosphere 208, 782–792. https://doi.org/10.1016/j.chemosphere.2018.06.031.

Otansev, P., Taskin, H., Bassari, A., Varinlioglu, A., 2016. Distribution and environmental impacts of heavy metals and radioactivity in sediment and seawater samples of the Marmara Sea. Chemosphere 154, 266–275. https://doi.org/10.1016/j.chemosphere.2016.03.122.

Paatero, P., 1997. Least squares formulation of robust non-negative factor analysis. Chemometr. Intell. Lab. 37, 23–35. https://doi.org/10.1016/S0169-7439(96)00044-5.

Paatero, P., Hopke, P.K., 2009. Rotational tools for factor analytic models. Chemometr. Intell. Lab. Syst. 23, 91–100. https://doi.org/10.1002/cem.1197.

Patel, P., Raju, N.J., Reddy, B.C.S.R., Suresh, U., Sankar, D.B., Reddy, T.V.K., 2018. Heavy metal contamination in river water and sediments of the Swarnamukhi River Basin, India: risk assessment and environmental implications. Environ. Geochem. Hlth. 40, 609–623. https://doi.org/10.1007/s10653-017-0006-7.

Pejman, A., Bidhendi, G.N., Ardestani, M., Saeedi, M., Baghvand, A., 2017. Fractionation of heavy metals in sediments and assessment of their availability risk: a case study in the northwestern of Persian Gulf. Mar. Pollut. Bull. 114, 881–887. https://doi.org/10.1016/j.marpolbul.2016.11.021.

Pueyo, M., Mateu, J., Rigol, A., Vidal, M., Lopez-Sanchez, J.F., Rauret, G., 2008. Use of the modified BCR three-step sequential extraction procedure for the study of trace element dynamics in contaminated soils. Environ. Pollut. 152, 330–341. https://doi.org/10.1016/j.envpol.2007.06.020.

Rosado, D., Usero, J., Morillo, J., 2015. Application of a new integrated sediment quality assessment method to Huelva estuary and its littoral of influence (Southwestern Spain). Mar. Pollut. Bull. 98, 106–114. https://doi.org/10.1016/j.marpolbul.2015.07.008.

Rodríguez Martín, J.A., Lopez-Arias, M., Grau Corbí, J.M., 2006. Heavy metals contents in agricultural topsoils in the Ebro basin (Spain). Application of the multivariate geoestatistical methods to study spatial variations. Environ. Pollut. 144, 1001–1012. https://doi.org/10.1016/j.envpol.2006.01.045.

Schwarz, J., Pokorna, P., Rychlik, S., Skachova, H., Vlcek, O., Smolik, J., Zdimal, V., Hunoval, I., 2019. Assessment of air pollution origin based on year-long parallel measurement of PM2.5 and PM10 at two suburban sites in Prague, Czech Republic. Sci. Total Environ. 664, 1107–1116. https://doi.org/10.1016/j.scitotenv.2019.01.426.

Shaike, M.M., Nath, B., Birch, G.F., 2014. Partitioning of trace elements in contaminated estuarine sediments: the role of environmental settings. Ecotox. Environ. Saf. 110, 246–253. https://doi.org/10.1016/j.ecoenv.2014.09.007.

Shomar, B., 2009. Source and buildup of Zn, Cd, Cr and Pb in the sludge of Gaza. Environ. Monit. Assess. 155, 51–62. https://doi.org/10.1007/s10661-008-0417-0.

Siddiqui, E., Pandey, J., 2019. Assessment of heavy metal pollution in water and surface sediment and evaluation of ecological risks associated with sediment contamination in the Ganga River: a basin-scale study. Environ. Sci. Pollut. Res. 26, 10926–10940. https://doi.org/10.1007/s11356-019-04495-6.

Soliman, N.F., Younis, A.M., Elkady, E.M., 2019. An insight into fraction, toxicity, mobility and source apportionment of metals in sediments from El Temsah Lake, Suez Canal. Chemosphere 222, 165–174. https://doi.org/10.1016/j.chemosphere.2019.01.009.

Song, H.Y., Hu, K.L., An, Y., Chen, C., Li, G.D., 2018. Spatial distribution and source apportionment of the heavy metals in the agricultural soil in a regional scale. J. Soil Sediment 18, 852–862. https://doi.org/10.1007/s11368-017-1795-0.

Sun, C.Y., Zhang, Z.X., Cao, H.N., Xu, M., Xu, L., 2019. Concentrations, speciation, and ecological risk of heavy metals in the sediment of the Songhua River in an urban area with petrochemical industries. Chemosphere 219, 538–545. https://doi.org/10.1016/j.chemosphere.2018.12.040.

Sundaray, S.K., Nayak, B.B., Lin, S., Bhatta, D., 2011. Geochemical speciation and risk assessment of heavy metals in the river estuarine sediments-a case study: Mahanadi basin, India. J. Hazard. Mater. 186, 1837–1846. https://doi.org/10.1016/j.jhazmat.2010.12.081.

Tessier, A., Campbell, P.G.C., Bisson, M., 1979. Sequential extraction procedure for the speciation of particulate trace metals. Anal. Chem. 51, 844–851. https://doi.org/10.1021/ac50043a017.

Toth, G., Hermann, T., Da Silva, M.R., Montanarella, L., 2016. Heavy metals in agricultural soils of the European Union with implications for food safety. Environ. Int. 88, 299–309. https://doi.org/10.1016/j.envint.2015.12.017.

U.S. Environmental Protection Agency EPA Positive Matrix Factorization (PMF) 5.0 Fundamentals and User Guide. Available at: https://www.epa.gov/sites/production/files/201502/documents/pmf_5.0_user_guide.pdf.

Unda-Calvo, J., Martinsz-Santos, M., Ruiz-Romera, E., 2017. Chemical and physiological metal bioaccessibility assessment in surface bottom sediments from the Deba River urban catchment: harmonization of PBET, TCLP and BCR sequential extraction methods. Ecotox. Environ. Safe. 138, 260–270. https://doi.org/10.1016/j.ecoenv.2016.12.029.

Wang, Q.H., Dong, Y.X., Zheng, W., Zhou, G.H., 2007. Soil geochemical baseline values and environmental background values in Zhejiang, China (in Chinese). Geol. Bull. China 26, 590–597.

Wang, Z.F., Zhou, J.Y., Zhang, C., Qu, L.Y., Mei, K., Dahlgren, R.A., Zhang, M.H., Xia, F., 2019a. A comprehensive risk assessment of metals in riverine surface sediments across the rural-urban interface of a rapidly developing watershed. Environ. Pollut. 245, 1022–1030. https://doi.org/10.1016/j.envpol.2018.11.078.

Wang, S., Cai, L.M., Wen, H.H., Jie, L., Wang, Q.S., Liu, X., 2019b. Spatial distribution and source apportionment of heavy metals in soil from a typical county-level city of Guangdong Province, China. Sci. Total Environ. 655, 92–101. https://doi.org/10.1016/j.scitotenv.2018.11.244.

Xia, F., Qu, L.Y., Wang, T., Luo, L.L., Chen, H., Dahlgren, R.A., Zhang, M.H., Mei, K., Huang, H., 2018. Distribution and source analysis of heavy metal pollutants in sediments of a rapid developing urban river system. Chemosphere 207, 218–228. https://doi.org/10.1016/j.chemosphere.2018.05.090.

Xue, J.L., Zhi, Y.Y., Yang, L.P., Shi, J.C., Zeng, L.Z., Wu, L.S., 2014. Positive matrix factorization as source apportionment of soil lead and cadmium around a battery plant (Changxing County, China). Environ. Sci. Pollut. Res. 21, 7698–7707. https://doi.org/10.1007/s11356-014-2726-x.

Zhang, G.L., Bai, J.H., Xiao, R., Zhao, Q.Q., Jia, J., Cui, B.S., Liu, X.H., 2017. Heavy metal fractions and ecological risk assessment in sediments from urban, rural and reclamation-affected rivers of the Pearl River Estuary, China. Chemosphere 184, 278–288. https://doi.org/10.1016/j.chemosphere.2017.05.155.

Zhao, K.L., Fu, W.J., Liu, X.M., Huang, D.L., Zhang, C.S., Ye, Z.Q., Xu, J.M., 2014. Spatial variation of concentrations of copper and its speciation in the soil-rice system in Wenling of southeastern China. Environ. Sci. Pollut. Res. 21, 7165–7176. https://doi.org/10.1007/s11356-014-2638-9.

Zhao, K.L., Fu, W.J., Qiu, Q.Z., Ye, Z.Q., Li, Y.F., Tunney, H., Dou, C.Y., Zhou, K.N., Qian, X.B., 2019. Spatial patterns of potentially hazardous metals in paddy soils in a typical electrical waste dismantling area and their pollution characteristics. Geoderma 337, 453–462. https://doi.org/10.1016/j.geoderma.2018.10.004.

Zhi, Y.Y., Li, P., Shi, J.C., Zeng, L.Z., Wu, L.S., 2016. Source identification and apportionment of soil cadmium in cropland of Eastern China: a combined approach of models and geographic information system. J. Soil Sediment 16, 467–475. https://doi.org/10.1007/s11368-015-1263-7.